

## Research Article

# Totally Ecofriendly Synthesis of Silver Nanoparticles from Aqueous Dissolutions of Polysaccharides

**M. A. Garza-Navarro,<sup>1,2</sup> J. A. Aguirre-Rosales,<sup>1</sup> E. E. Llanas-Vázquez,<sup>1</sup>  
I. E. Moreno-Cortez,<sup>1,2</sup> A. Torres-Castro,<sup>1,2</sup> and V. González-González<sup>1,2</sup>**

<sup>1</sup> *Universidad Autónoma de Nuevo León, Facultad de Ingeniería Mecánica y Eléctrica, Avenida Universidad S/N, Ciudad Universitaria, 66450 San Nicolás de los Garza, NL, Mexico*

<sup>2</sup> *Universidad Autónoma de Nuevo León, Centro de Innovación, Investigación y Desarrollo en Ingeniería y Tecnología, 66450 Apodaca, NL, Mexico*

Correspondence should be addressed to A. Torres-Castro; [alejandro.torrescs@uanl.edu.mx](mailto:alejandro.torrescs@uanl.edu.mx)

Received 5 June 2013; Revised 6 September 2013; Accepted 7 September 2013

Academic Editor: Shaojun Li

Copyright © 2013 M. A. Garza-Navarro et al. This is an open access article distributed under the Creative Commons Attribution License, which permits unrestricted use, distribution, and reproduction in any medium, provided the original work is properly cited.

In this contribution, a totally ecofriendly synthesis of silver nanoparticles from aqueous dissolution of polysaccharides is reported. The synthesis of nanoparticles was performed using aqueous dissolutions of silver nitrate ( $\text{AgNO}_3$ ) and carboxymethyl-cellulose (CMC) as both reducing and stabilization agent and using different  $\text{AgNO}_3$  : CMC weight ratios. Resultant yellowish to reddish dispersions were characterized by means of transmission electron microscopy and their related techniques, such as bright field and Z-contrast imaging and electron diffraction, as well as ultraviolet-visible and infrared spectroscopic techniques. The experimental evidence suggests that the morphology and particle size distribution of the silver nanoparticles depend on the  $\text{AgNO}_3$  : CMC weight ratio. This feature seems to be related to the stabilization given by the CMC matrix, which, according to our experimental findings, is steric in nature. Regarding such experimental evidence, a synthesis mechanism in which CMC acts as stabilizer and reducing agent is proposed.

## 1. Introduction

The synthesis of metal nanostructures has been extensively studied due to their potential applications in technological fields such as electronics, optics, and medicine [1–3]. Accordingly, silver nanoparticles (AgNPs) are a promising nanostructured system, due to its potential to be applied as bactericide, fungicide, and antiviral [4–6]. Several approaches have been suggested for the synthesis of silver nanoparticles. These approaches propose the preparation of silver nanoparticles into alkaline or acidic media and using toxic reagents, such as sodium borohydride ( $\text{NaBH}_4$ ), N, N-dimethylformamide, or hydrazine, as reducing reactants, or ionic surfactants as cetyltrimethylammonium bromide (CTAB) and polyvinylpyrrolidone as stabilization agents [1–12]. Nevertheless, these routes generate residues that involved environmental risks.

Therefore, in order to minimize the environmental impact of the synthetic processes for the development of nanostructures, green chemistry routes must be adopted. As one can find in the literature, the synthetic methods that evoke green preparation of silver nanoparticles and other metal nanoparticles consider biopolymers such as chitosan, carboxymethyl-chitosan, carboxymethyl-cellulose, or water-soluble starch as both reducing and stabilization agents [11–15].

Among these polymers, the polysaccharide carboxymethyl-cellulose (CMC) has emerged as an important stabilization and/or reducing reagent. The CMC is a semisynthetic polysaccharide, derived from the natural polymer cellulose, which undergoes the partial substitution of cellulose native hydroxyl-methyl groups by carboxy-methyl groups [16]. The degree of substitution (DS) of these functional groups is usually reported as an average of carboxy-methyl groups per

monomer unit. Due to this substitution, the CMC has a polyelectrolyte character, being a polyanion at pH above 4, whereas below this value carboxylic anions are protonated. The CMC is commercialized as water-soluble sodium salt (NaCMC), which in aqueous dissolution can be loaded with metallic ions by a simple displacement reaction of sodium cations [17]. Regarding this feature, the synthesis of hybrid materials based on Cu, Fe, and Ag nanoparticles stabilized into CMC matrix, departing from coordination complex between this last and the, respectively, metal cations has been possible [17–20]. Moreover, due to the abundant hydroxyl groups on its molecular structure, CMC can be also used as both stabilization and reducing agent for the preparation of metal nanoparticles like Au, Pd, Pt, and Ag [17–19].

Herein, we propose a simple one-pot totally eco-friendly approach for the preparation of AgNPs, from aqueous dissolutions of the polysaccharide CMC as reducing and stabilization media, that do not use nor produce any harmful residue. Following this route, it is safe to use high concentrations of CMC for the efficient reduction of silver ions in aqueous dissolutions and to give narrow particle size distribution of AgNPs, even at lower  $\text{AgNO}_3/\text{CMC}$  weight ratios than that reported in the literature [9, 15]. Moreover, unlike other reports regarding the synthesis of such nanostructures, even those that are microwave-assisted [14, 15, 17], using this synthetic approach makes it possible to get an outstanding control over the size of the AgNPs and their distribution, and remarkable efficiency over the silver reduction. Finally, the proposed approach is simpler than any other one nowadays reported in the literature, and hence, could be easily industrially scalable for the mass production of AgNPs.

## 2. Materials and Methods

**2.1. Materials.** For this research, reagents as silver nitrate ( $\text{AgNO}_3$ ) and CMC ( $M_w = 250$  kDa,  $DS = 1.2$ ) were acquired from Sigma-Aldrich Co. and used as received without further treatment.

**2.2. Synthesis Procedure.** Aqueous dissolutions of CMC and  $\text{AgNO}_3$  were prepared using deionized water, which was obtained from a Barnstead EASYpure II system with  $\rho = 18$  M $\Omega$ -cm and pH of 6.98. The CMC and  $\text{AgNO}_3$  dissolutions were prepared using concentrations of 15 mg/mL and 9.64 mg/mL, respectively. The  $\text{AgNO}_3$  dissolution was diluted at necessary concentration to obtain samples at  $\text{AgNO}_3/\text{CMC}$  weight ratios of  $0.8 \times 10^{-3}$ ,  $1.6 \times 10^{-3}$ ,  $3.1 \times 10^{-3}$ , and  $4.2 \times 10^{-3}$ ; these samples were identified as AgCMC1, AgCMC2, AgCMC3, and AgCMC4, respectively. The proposed green chemistry approach for the preparation of materials based on silver nanoparticles and CMC was carried out as follows. First, 20 mL of the CMC aqueous dissolution was placed at room temperature into a 100 mL round-bottom three-neck flask and stirred for 10 minutes. Later, 10 mL of  $\text{AgNO}_3$  aqueous dissolution was added to the reactor and the temperature of the reactor was quickly raised to 90°C and kept in that way for 24 hours under reflux condition. Once the reaction time elapsed, resultant yellowish to reddish

dissolutions (depending on the Ag:CMC weight ratio) were quickly placed into a previously cooled 50 mL round-bottom flask, in order to rapidly cool it down to room temperature. Finally, the samples were diluted to a known concentration to give a final dissolution volume of 50 mL and collected for their subsequent characterization.

**2.3. Characterization.** Crystalline and morphological characteristics of the samples were studied by transmission electron microscopy (TEM) using a FEI TITAN G<sup>2</sup> 80–300 and employing electron microscopy (EM) techniques such as bright field (BF) and Z-contrast (STEM) imaging, as well as selected area electron diffraction (SAED). In order to characterize the synthesized samples using these EM techniques, the specimens were prepared using diluted dispersions (20% v/v) of the samples that were placed onto carbon-coated grids (EMS, lacey-carbon copper grids). The formation of AgNPs was evaluated by ultraviolet-visible (UV-vis) spectroscopy using a Perkin-Elmer Lambda 35 spectrometer. For this study, 4 mL of the diluted dispersions was directly placed into Perkin Elmer quartz-cells (part no. B0631009) without further treatment. The interactions between CMC functional groups and the synthesized nanoparticles were evaluated by Fourier transform infrared spectroscopy (FTIR) using a Thermo-Scientific Nicolet spectrometer. In this case, the preparation of the specimens was performed as follows: 6 drops of diluted dispersions of the samples were added to 60 mg of powdered potassium bromide (KBr, FTIR grade  $\geq 99\%$ ), mixed, and dried at 60°C for 24 hours. Dried mixtures were pressed to get films of the specimens, from which the IR spectra were recorded.

## 3. Results and Discussion

**3.1. Crystalline and Morphological Characterization.** Figure 1 shows EM images obtained from samples AgCMC1, AgCMC2, AgCMC3, and AgCMC4 using STEM technique. As one can see, all samples display the presence of quasispherical nanoparticles (brighter regions), which seem to be embedded into a noncrystalline matrix (darker regions around particles). Moreover, the particle size and distribution change as the concentration of  $\text{AgNO}_3$  increases (see the graphs of particle size distribution on the right-hand side of each STEM image). As the concentration of the  $\text{AgNO}_3$  increases the central value ( $\mu$ ) seems to increase as well as the width of distribution ( $\sigma$ ). It is worth mentioning that these distribution curves were obtained from the measuring of around 500 particles in each sample.

On the other hand, Figure 2 shows high magnification BF images obtained from samples AgCMC1, AgCMC2, AgCMC3, and AgCMC4 along with its correspondent SAED pattern. BF images show that the nanoparticles depict regular crystalline arrangements, which, according to the interplanar measuring (showed in the figures), can be related to that reported for the family planes {311} of silver (see JCPDS: 04-0783). The crystalline structure of nanoparticles is corroborated by the SAED patterns obtained from these samples, since it can identified diffraction rings related to the family planes {111}, {200}, {220}, and {311} reported for silver.

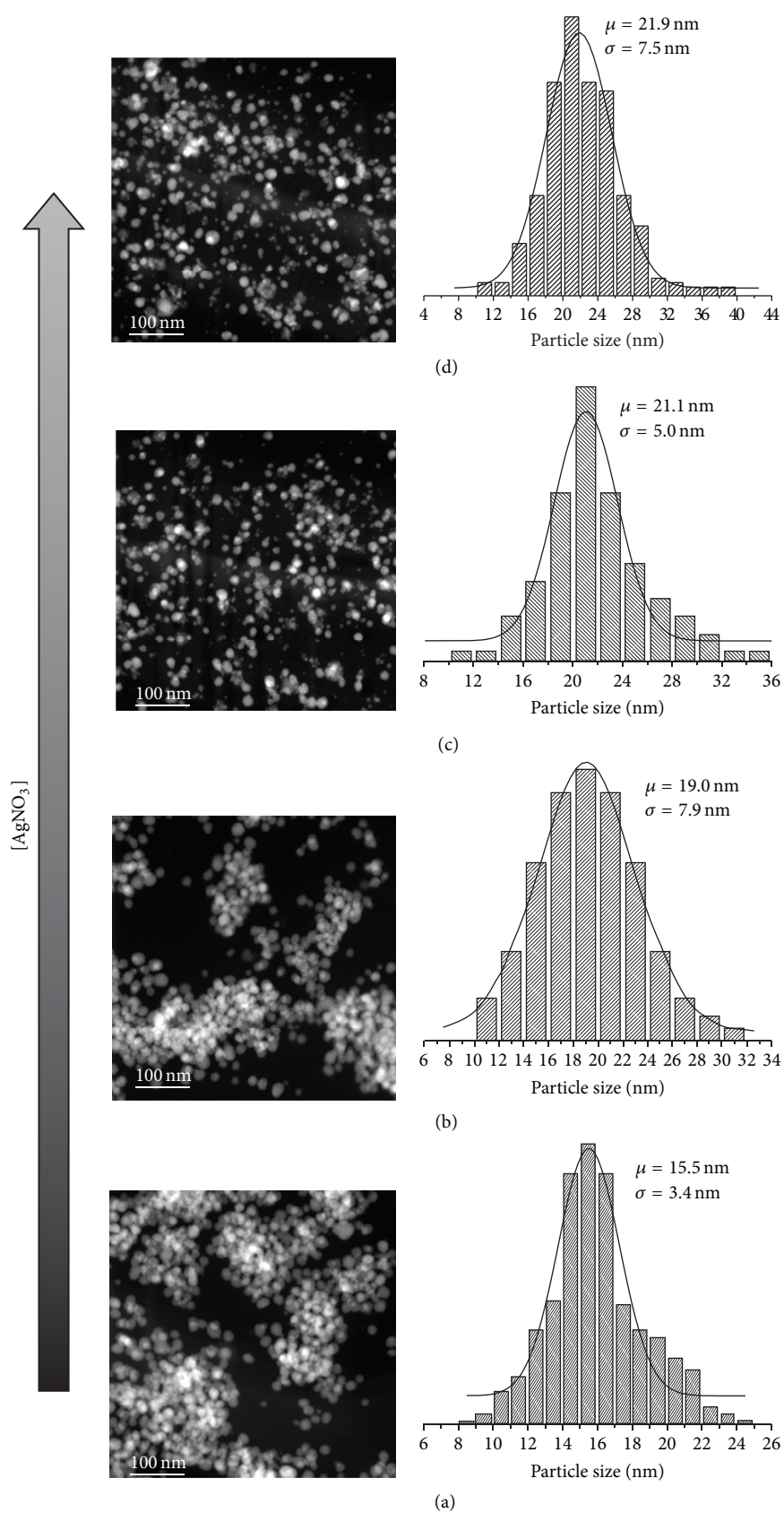


FIGURE 1: STEM images that show the morphological characteristics of the samples: (a) AgCMC1, (b) AgCMC2, (c) AgCMC3, and (d) AgCMC4, along with their correspondent particle size distribution. The distribution graph of each sample is located on the right hand of its correspondent STEM image.



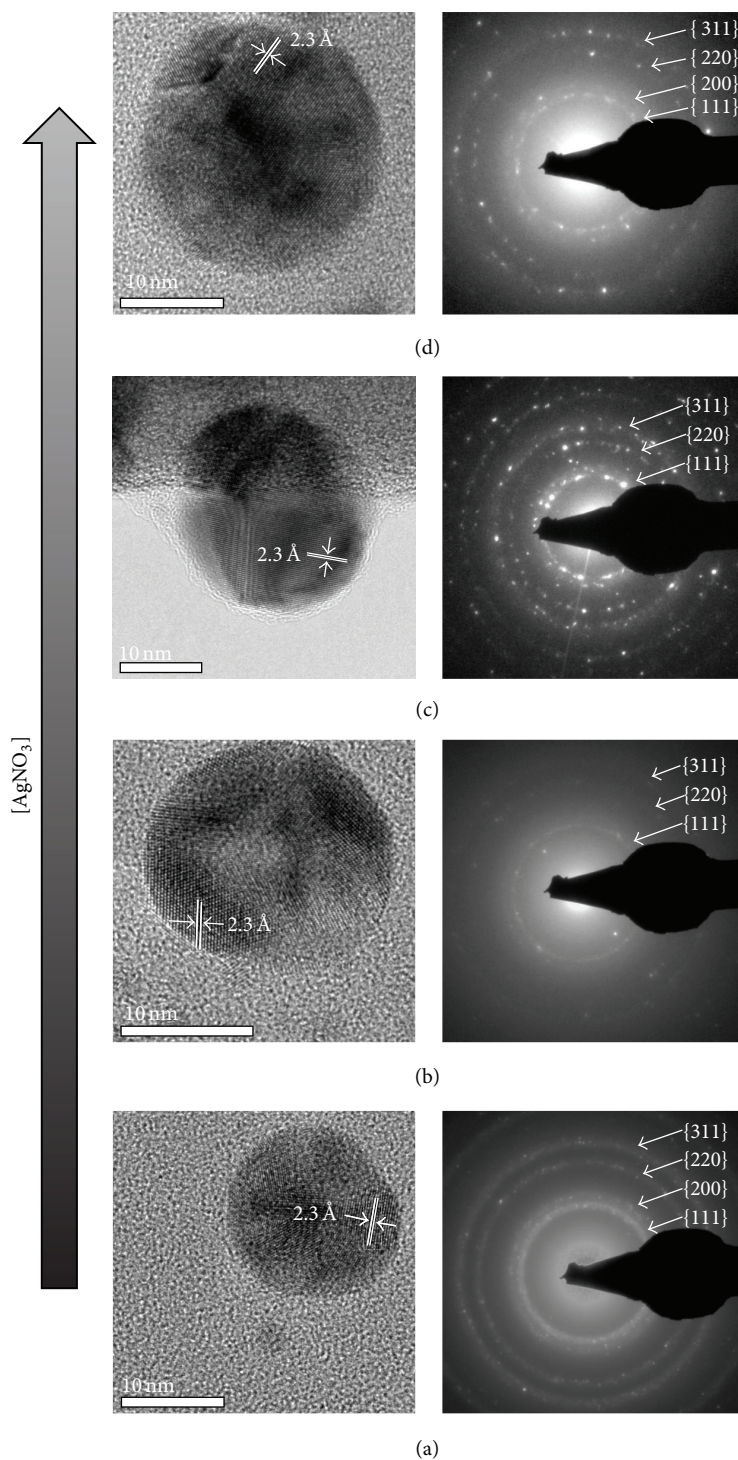


FIGURE 2: High magnification BF images that show nanoparticles of the samples: (a) AgCMC1, (b) AgCMC2, (c) AgCMC3, and (d) AgCMC4, along with their correspondent SAED pattern. The SAED pattern of each sample is located on the right hand of its correspondent BF image.

From these results, it is possible to assume that the size and distribution of the silver nanoparticles depend on the  $\text{AgNO}_3$  : CMC weight ratio that is used for the synthesis of each sample, although its morphology seems to be independent of such ratio. This feature could be related to the nature of the stabilization given by the CMC matrix. Accordingly,

assuming that all  $\text{Ag}^+$  ions are reduced to  $\text{Ag}^0$ , the increase in the content of silver atoms could start to diminish the ability of CMC to avoid the particles aggregation and its secondary growth. However, in order to know if all silver ions are reduced into  $\text{Ag}^0$  in our samples and to elucidate if this feature diminishes the ability of CMC matrix to avoid the

particles aggregation, we proceed to characterize the samples by means of spectroscopic techniques, such as UV-vis and FTIR.

**3.2. Spectroscopic Characterization.** Figure 3 shows the UV-vis spectra obtained from samples AgCMC1, AgCMC2, AgCMC3, and AgCMC4, as well as that measured from the  $\text{AgNO}_3$  aqueous dissolution used as reagent for its synthesis (AgSOL). As one can see, the samples' spectra do not show absorption bands related to the  $\text{Ag}^+$  ions at 301 nm, as the AgSOL spectrum does. Instead, there are well defined bands with maximum around 400 nm; as has been previously reported, this band can be assigned to the collective resonance of electrons at the surface of the silver nanoparticles (surface plasmon resonance (SPR)) [9, 21, 22].

These results indicate that, in all cases, it was possible to reach a full reduction of the added  $\text{Ag}^+$  ions during the reaction. Accordingly, the concentration of silver nanoparticles in the samples, AgCMC1, AgCMC2, AgCMC3, and AgCMC4, can be calculated as 50 ppm, 100 ppm, 200 ppm, and 267 ppm, respectively. Moreover, it is possible to notice that the maximum of these bands shows a bathochromic shift, and that its width increases as the concentration of  $\text{AgNO}_3$  in the reaction does. This feature can be explained as follows [23]. SPR results from the synchronic vibration of a large number of conduction electrons at the surface of metal nanoparticles. Such vibration can be activated from electromagnetic stimuli, as in the case of the photons transferring its lineal momentum to these "free electrons." However, the magnitude of the energy that is needed to activate this process depends on the confinement degree of electrons. As it is known, significant electronic confinement phenomena can be observed in nanoparticles, since the number of atoms that composed them is reduced. Thus, the density of electronic states of the nanostructures is lower than that expected for its massive counterpart. This means that the degree of the electronic confinement in nanostructures mainly depends on their size and shape.

Therefore, the progressive bathochromic shift of the bands, related to the SPR in our samples, can be understood as an increase of the particle size, as the concentration of  $\text{AgNO}_3$  in the reaction increases. In addition, the increase in the width of the SPR bands can be associated with the increase in the particle size distribution of samples [9, 13, 21–23]. It is worth mentioning that these results are congruent with those obtained from the crystalline and morphological characterization of our samples.

Figure 4 shows the FTIR spectra obtained from the synthesized samples as well as that measured from as-received CMC. In the spectra, it can be noticed that bands are attributable to the vibration of functional groups of CMC, as has been reported elsewhere [17–19]. These bands can be assigned as follows: the band at  $3434\text{ cm}^{-1}$  corresponds to the symmetrical and asymmetrical stretching at the O–H bond of the hydroxyl groups (R–OH); the band at  $2926\text{ cm}^{-1}$  is associated with the asymmetrical stretching at the C–H bond of the hydroxyl-methyl functional groups (R–CH<sub>2</sub>OH); bands at  $1600\text{ cm}^{-1}$  and  $1420\text{ cm}^{-1}$  are related to the asymmetrical and symmetrical, respectively, stretching vibration at the

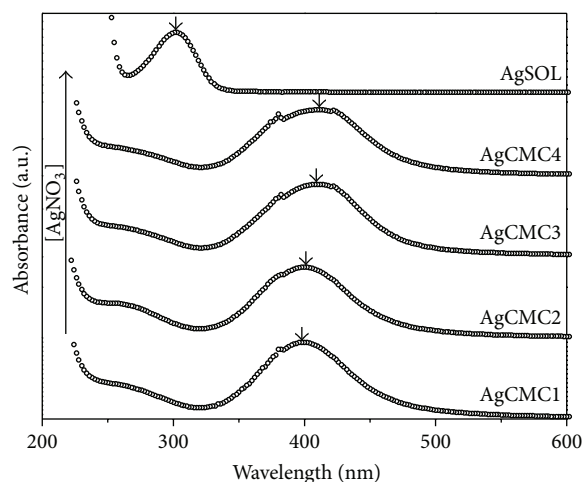


FIGURE 3: UV-vis spectra obtained from samples AgCMC1, AgCMC2, AgCMC3, AgCMC4, and AgSOL.

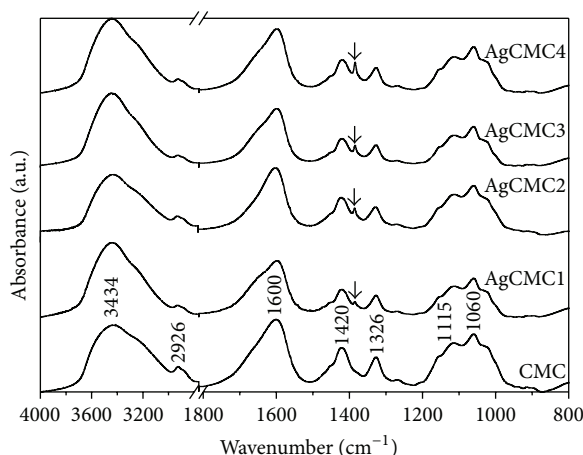


FIGURE 4: FTIR spectra obtained from the samples AgCMC1, AgCMC2, AgCMC3, and AgCMC4, as well as that recorded from native CMC.

–O–C=O bonds on the carboxy-methyl functional groups (R–CH<sub>2</sub>OCOO–); the band at  $1326\text{ cm}^{-1}$  is assigned to the bending vibration at –C–CH and O–CH– bonds on the R–CH<sub>2</sub>OCOO– groups; and finally, bands at  $1115$  and  $1060\text{ cm}^{-1}$  are attributed to the stretching vibration at C–O and C–O–C bonds, respectively, on R–CH<sub>2</sub>OCOO– functional groups.

In addition, as Figure 4 shows, FTIR spectra of the samples display a band at  $1385\text{ cm}^{-1}$ , which, according to the literature, can be assigned to the symmetrical stretching vibration at O–N–O bond on the nitrate radical ( $\text{O}=\text{NO}_2^-$ ) [24, 25]. The apparition of such band suggests the formation of an inorganic salt between the sodium cations, which were displaced from its native position at R–CH<sub>2</sub>OCOO– groups of CMC, and those nitrate anions from the  $\text{AgNO}_3$  reagent employed in the synthesis of the nanoparticles. Although the formation of such inorganic salt seems to be feasible, the fact that the spectra present no shifts on the position of bands related to vibrations at R–CH<sub>2</sub>OCOO– groups, with

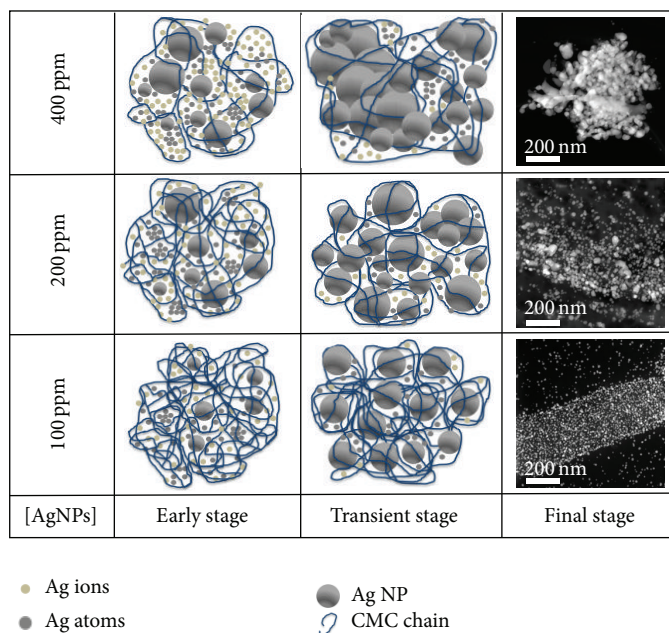


FIGURE 5: Schematic that represents the proposed mechanism for the synthesis of AgNPs, in which the CMC acts as stabilizer and reducing agent.

respect to the position of such vibration in the as-received CMC spectrum, suggests that most of the sodium cations remain on its native position once the synthesis elapsed. This implies that the stabilization given by the CMC matrix is steric in nature, since there is not experiment evidence pointing to the adsorption of CMC chain onto synthesized silver nanoparticles, as it has been reported for other metal nanoparticles systems [18, 19].

Thus, the silver nanoparticles nucleate and grow at intermolecular sites among CMC chains, but these chains are not adsorbed onto nanoparticles' surface. Once these sites are saturated, the secondary growth can happen among well-dispersed nanoparticles and those nanoparticles that are nucleating and growing close to them. It is worth mentioning that the experimental evidence about the morphological characteristics of the synthesized samples supports this feature.

### 3.3. Mechanism for the Formation of the Silver Nanoparticles.

As one can find in the literature, several approaches have used hydroxylated polymer, such as polysaccharides and their derivatives, for the synthesis and stabilization of metal nanoparticles [11–13]. Specifically, the polysaccharide CMC is able to form coordination complexes between its carboxylate radicals and transition metal cations (i.e., Fe and Cu) or with some noble and semionoble transition metal cations (i.e., Au, Pd, Pt, and Ag) [17–20]. This feature promotes the attraction of the metal cations to intermolecular sites nearby the negatively charged  $\text{R-CH}_2\text{OCOO}^-$  groups of the CMC, when both are diluted in aqueous media [17–19]. Such attraction results from the displacement of native sodium ions from carboxylate functional groups and replacement with transition metal cations [17].

In our case, once the silver cations are attracted to the aforementioned intermolecular sites of the CMC, the temperature of the aqueous medium is raised above  $80^\circ\text{C}$ , which induced thermal vibrations that couple with the polar hydroxyl groups ( $\text{R-OH}$  or  $\text{R-CH}_2\text{OH}$ ) of  $\beta$ -glucopyranose units. This coupling conduces to the release of electrons from these groups and the subsequent reduction of metal cations [9, 17]. Thus, reduced silver ions, dispersed into the medium, act as nucleation centers and catalyze the reduction of other cations around them [9]. Then, the coalescence of atoms nearby the nucleation centers promotes the formation of silver metal clusters and the addition of silver cations onto its surface, which are subsequently reduced. This process continues until an elevated number of nuclei are reached, which depends on the quantity of reactant added to the reaction. This phenomenon is illustrated in Figure 5 as the early stage of the synthesis of the silver nanoparticles. As it can be found in the literature, this process can be accelerated by the addition of alkali dissolutions to the reaction or by the microwave-assisted heating of the reaction [9, 15]. Nonetheless, addition of alkali dissolutions to the reaction generates harmful residues that involve environmental risks, which we avoid using only CMC. On the other hand, microwave-assisted heating of the reaction leads to the formation of undesirable silver compounds, when low  $\text{AgNO}_3/\text{CMC}$  weight ratios are used (as low as that used in this investigation).

However, the carboxylic groups are not capable of making strong bonds with the surface of noble or semionoble metal nanoparticles, since the average charge on its surface is zero [17, 25]. Accordingly and as our experimental evidence suggests, effective adsorption of CMC onto silver nanoparticles does not occur. Instead, the stabilization mechanism to avoid the secondary growth seems to be related to the CMC chains wrapping the silver nanoparticles. This feature is illustrated in



Figure 5 as transient stage of the synthesis mechanism of our samples.

Therefore, as silver nanoparticles weight content increase, there is an increase in the probability that the particles collide in the reaction medium, leading to the formation of nanoparticles aggregates. This feature is illustrated in Figure 5 as a final stage in the synthesis of our samples. Moreover, as one can see in these STEM images, when the silver nanoparticles concentration increases above 200 ppm (i.e., 400 ppm, as is shown in the figure), particles aggregation conduces to the formation of silver rod-like structures. This phenomenon enforces the hypothesis regarding the fact that the stabilization given by CMC for the control of particle size is steric in nature, but also points to the fact that its intermolecular sites act as a template for the formation of this kind of nanostructures, as it has been reported elsewhere [26].

#### 4. Conclusions

The totally eco-friendly synthesis of silver nanoparticles from aqueous dissolution of polysaccharides was demonstrated. The synthesized silver nanoparticles display a quasi-spherical morphology, according to the micrographs obtained from STEM technique. In addition, the BF images and the SAED patterns identify the crystalline arrangement present in the synthesized nanoparticles as that reported for silver. The UV-vis spectra obtained from the synthesized samples show absorption band around 400 nm, which is characteristic of the SPR of silver nanoparticles. The FTIR spectra confirmed that the stabilization given by the matrix is steric in nature, since the spectra of the samples did not show any change on the position of the characteristic vibration bands of the CMC. Furthermore, on the basis of the experimental evidence, a synthesis mechanism in which the CMC acts as stabilizer and reducing agent, preventing the excessive agglomeration of the AgNPs, is proposed. Finally, it is worth mentioning that this work has settled the principles for future developments in the fabrication of nanoparticles using green chemistry approaches that can be industrially scalable for the mass production of AgNPs.

#### References

- [1] P. K. Jain, X. Huang, I. H. El-Sayed, and M. A. El-Sayed, "Noble metals on the nanoscale: optical and photothermal properties and some applications in imaging, sensing, biology, and medicine," *Accounts of Chemical Research*, vol. 41, no. 12, pp. 1578–1586, 2008.
- [2] X. Wang, C. Wang, L. Cheng, S.-T. Lee, and Z. Liu, "Noble metal coated single-walled carbon nanotubes for applications in surface enhanced Raman scattering imaging and photothermal therapy," *Journal of the American Chemical Society*, vol. 134, pp. 7414–7422, 2012.
- [3] R. Brenier, "Enhancement of light transmission through silver nanoparticles," *Journal of Physical Chemistry C*, vol. 116, no. 9, pp. 5358–5366, 2012.
- [4] L. Wang, J. Luo, S. Shan et al., "Bacterial inactivation using silver-coated magnetic nanoparticles as functional antimicrobial agents," *Analytical Chemistry*, vol. 83, no. 22, pp. 8688–8695, 2011.
- [5] R. Prucek, J. Tucek, M. Kilianová et al., "The targeted antibacterial and antifungal properties of magnetic nanocomposite of iron oxide and silver nanoparticles," *Biomaterials*, vol. 32, pp. 4704–4713, 2011.
- [6] A. Panáček, M. Kolář, R. Večeřová et al., "Antifungal activity of silver nanoparticles against *Candida* spp," *Biomaterials*, vol. 30, no. 31, pp. 6333–6340, 2009.
- [7] O. Soltwedel, O. Ivanova, M. Höhne, M. Gopinadhan, and C. A. Helm, "Aggregation and rearrangement within a silver nanoparticle layer during polyelectrolyte multilayer formation," *Langmuir*, vol. 26, no. 19, pp. 15219–15228, 2010.
- [8] Y. Murali Mohan, K. Vimala, V. Thomas et al., "Controlling of silver nanoparticles structure by hydrogel networks," *Journal of Colloid and Interface Science*, vol. 342, no. 1, pp. 73–82, 2010.
- [9] A. A. Hebeish, M. H. El-Rafie, F. A. Abdel-Mohdy, E. S. Abdel-Halim, and H. E. Emam, "Carboxymethyl cellulose for green synthesis and stabilization of silver nanoparticles," *Carbohydrate Polymers*, vol. 82, no. 3, pp. 933–941, 2010.
- [10] D. K. Bhui and A. Misra, "Synthesis of worm like silver nanoparticles in methyl cellulose polymeric matrix and its catalytic activity," *Carbohydrate Polymers*, vol. 89, pp. 830–835, 2012.
- [11] S. M. Ghaseminezhad, S. Hamed, and S. A. Shojaosadati, "Green synthesis of silver nanoparticles by a novel method: comparative study of their properties," *Carbohydrate Polymers*, vol. 89, pp. 467–472, 2012.
- [12] M. J. Laudenslager, J. D. Schiffman, and C. L. Schauer, "Carboxymethyl chitosan as a matrix material for platinum, gold, and silver nanoparticles," *Biomacromolecules*, vol. 9, no. 10, pp. 2682–2685, 2008.
- [13] E. A. Venediktov and V. A. Padokhin, "Synthesis of silver nanoclusters in starch aqueous solutions," *Russian Journal of Applied Chemistry*, vol. 81, no. 11, pp. 2040–2042, 2008.
- [14] K. J. Sreeram, M. Nidhin, and B. U. Nair, "Microwave assisted template synthesis of silver nanoparticles," *Bulletin of Materials Science*, vol. 31, no. 7, pp. 937–942, 2008.
- [15] J. Chen, J. Wang, X. Zhang, and Y. Jin, "Microwave-assisted green synthesis of silver nanoparticles by carboxymethyl cellulose sodium and silver nitrate," *Materials Chemistry and Physics*, vol. 108, pp. 421–424, 2008.
- [16] T. Chakraborty, I. Chakraborty, and S. Ghosh, "Sodium carboxymethylcellulose. CTAB interaction: a detailed thermodynamic study of polymer: surfactant interaction with opposite charges," *Langmuir*, vol. 22, no. 24, pp. 9905–9913, 2006.
- [17] M. N. Nadagouda and R. S. Varma, "Synthesis of thermally stable carboxymethyl cellulose/metal biodegradable nanocomposites for potential biological applications," *Biomacromolecules*, vol. 8, no. 9, pp. 2762–2767, 2007.
- [18] J. Liu, F. He, T. M. Gunn, D. Zhao, and C. B. Roberts, "Precise seed-mediated growth and size-controlled synthesis of palladium nanoparticles using a green chemistry approach," *Langmuir*, vol. 25, no. 12, pp. 7116–7128, 2009.
- [19] F. He, D. Zhao, J. Liu, and C. B. Roberts, "Stabilization of Fe-Pd nanoparticles with sodium carboxymethyl cellulose for enhanced transport and dechlorination of trichloroethylene in soil and groundwater," *Industrial and Engineering Chemistry Research*, vol. 46, pp. 29–34, 2007.
- [20] F. He and D. Zhao, "Manipulating the size and dispersibility of zerovalent iron nanoparticles by use of carboxymethyl cellulose stabilizers," *Environmental Science and Technology*, vol. 41, no. 17, pp. 6216–6221, 2007.

- [21] P. Raveendran, J. Fu, and S. L. Wallen, "Completely "Green" synthesis and stabilization of metal nanoparticles," *Journal of the American Chemical Society*, vol. 125, no. 46, pp. 13940–13941, 2003.
- [22] M. M. Kemp, A. Kumar, S. Mousa et al., "Synthesis of gold and silver nanoparticles stabilized with glycosaminoglycans having distinctive biological activities," *Biomacromolecules*, vol. 10, no. 3, pp. 589–595, 2009.
- [23] P. Mulvaney, "Surface plasmon spectroscopy of nanosized metal particles," *Langmuir*, vol. 12, no. 3, pp. 788–800, 1996.
- [24] B. D. Mistry, *A Handbook of Spectroscopic Data*, Oxford Book Company, New Delhi, India, 2009.
- [25] T. R. Kozlowski and R. F. Bartholomew, "Reactions between sodium carboxylic acid salts and molten sodium nitrate and sodium nitrite," *Inorganic Chemistry*, vol. 7, no. 11, pp. 2247–2254, 1968.
- [26] J. Tan, R. Liu, W. Wang et al., "Controllable aggregation and reversible pH sensitivity of AuNPs regulated by carboxymethyl cellulose," *Langmuir*, vol. 26, no. 3, pp. 2093–2098, 2010.



